ORIGINAL ARTICLE

The effect of laser beam wobbling mode in welding process for structural steels

Sergey V. Kuryntsev[1] · A. Kh. Gilmutdinov[1]

Abstract A laser welding process using a 30-kW fiber laser with scanning mode optics is investigated in the paper. Welding is conducted in two ways: constant laser beam trajectory and wobbling trajectory with the use of lower speed and power. The main goal was to investigate the influence of the second wobbling laser welding pass on microstructure and mechanical properties of structural steel. The following parameters were monitored: visual control and mechanical properties (microhardness, three-point bend, and Charpy impact V-notch test); metallographic analysis and 2D and 3D computer tomography (CT) were also done. The results show that after the second welding pass, with wobbling trajectory of laser beam, middle and cap parts of the seam have a lower microhardness, in relation to the root part. It can be explained by annealing influence of the second wobbling pass at weld metal.

Keywords Wobbling beam trajectory · Fiber laser welding · Mechanical properties · Ductility · Microhardness · Computer tomography · Microstructure

✉ Sergey V. Kuryntsev
kuryntsev16@mail.ru

[1] Kazan National Research Technical University named after A.N. Tupolev-KAI (KNRTU-KAI), Kazan, Russia

1 Introduction

In the last few years, lot of papers about laser welding with special technical applications, like hybrid laser arc welding [1–6], twin spot laser welding, laser welding with cold filler material [6], friction stir welding with laser tempering, hybrid welding with different combination arc leading, laser leading etc., were published. In addition, hybrid laser welding is used for dissimilar materials, like Fe–Al joint [7], bifocal laser beam welding "turbo-weld" for specimen with different thicknesses [8].

Laser welding is a very popular joint process, due to high welding speed, smaller heat-affected zone (HAZ), low deformation, and other aspects, but very high cooling rates result in the formation of hardening structures that increases hardness, decreases plasticity of weld joint and HAZ, and increases the level of residual stresses. Original laser welding of thick and long plates requires final preparation, alignment, fixation, and welding process control. This problem can be solved using twin spot laser technique with filler wire or hybrid arc-laser welding [6–14], but it will decrease the welding speed. One of the ways to solve this problem is the use of a laser beam wobbling mode.

Classical technology of reducing hardness of the welded joint is preheating before welding or heat treatment after welding [15–17]. Currently, however, there are technological solutions that reduce hardness of the weld joints during the welding process, such as defocused laser beam welding, bifocal beam, or laser-arc welding. The authors [18] use two-pass method or heat treatment of the whole weld for reducing hardness of the welded joint obtained by laser-arc welding of martensitic steel. Two-pass method can reduce the temperature of preheating by 100 °C; the authors note that, in laser welding of large thickness, there is high hardness of the weld root side in

one pass observed, which is associated with a higher heat loss in comparison with the cap side.

In the works [19, 20], experiments on defocused beam laser welding are described; it gives opportunity to increase the weld pool, reduce the solidification rate, reduce hardness of the weld metal, and reduce the probability of solidification cracks.

In the present work, the influence of the second welding pass with laser beam wobbling on mechanical properties of welding seam and HAZ for structural steels was studied. Using this technique, one can significantly increase plasticity and toughness and make hardness of welding seam and HAZ more homogeneous.

2 Experiment

For the welding experiment, a five-axis robot KUKA KR 120 R 2700 extra HA, fiber laser LS-30 of "IPG—Photonics" (USA) were used as a heat source; welding laser focusing head with line scan unit LK-690 (KUGLER GmbH) was applied. The wave length of the fiber laser is 1070 nm; focal length is 450 mm. The defocusing distance of laser beam to the surface of workpiece is 0.0 mm, laser spot diameter in focus is 200 μm, 99.99 % purity argon was used as a shielding gas to protect the top part of molten pool, and distance between shielding tubes and surface of workpiece is 1.0–1.2 mm. The flow rate of shielding gas is 20 l/min. The chemical composition of the welded workpieces are presented in Table 1; the specimen before welding is 10 mm thick, 50 mm wide, and 200 mm long. Type 321S12 stainless steel (sample 1), 1449-27/23CR structural steel (samples 2 and 3), and 9MnSi5 low-alloy steel (samples 4 and 5) were investigated.

To investigate the influence of laser beam wobbling mode on the mechanical properties and microstructure, wobbling frequency, emission power, and welding speed of the second welding pass were varied. Welding was performed in two passes: the first pass was at the speed of 15–36 mm/s and laser power of 8–12,5 kW, without wobbling of laser beam (Fig. 1a), and the second pass was at the speed of 8–10 mm/s and laser power of 3–4 kW with wobbling of laser beam
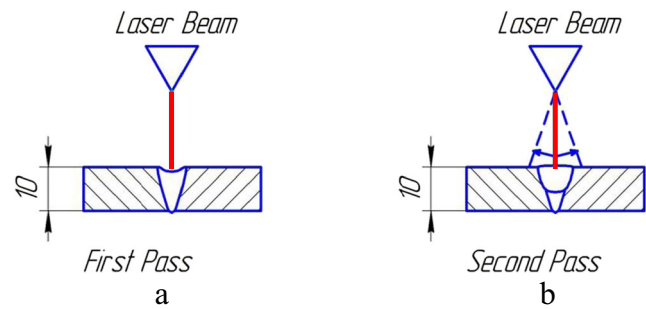
Fig. 1 Schematic view of the **a** first and **b** second welding pass

transverse to the direction of welding (Fig. 1b) at a certain frequency and amplitude (Table 2).

Welding parameters are presented in Table 2. The welding process was made based on a written program for the robot, i.e., after the first weld pass, the robot returned to the starting point of the first pass and began the second pass over the first one. Thus, it turns out that, during the second pass, the weld metal of the first pass remelted, removing defects such as undercuts and weld nonuniformity in height. The depth of the remelted metal was about 3–4 mm (Fig. 4). For the stainless steel, two-sided welding or "turbo-weld" [8] with beam wobbling mode with the same parameters was used; it is due to very high thermal distortion of that type of steel [1] that welding was done without use of shielding gas. Usually, stainless steels have a high level of thermal distortion; it is explained by phase and structural transition processes. In our experiment, we use double-side laser beam welding, by similar welding parameters of Table 2. After the first welding pass, thermal deformation of workpieces was observed; there is an angle about 170° between them. The second welding pass compensated for the distortion and deformation after the first welding pass.

To reveal the microstructure, an etchant of solution of 5 % nitric acid in alcohol was used. For the investigation of the microstructure, an optical microscope Axiovert Observer.D1m of "Carl Zeiss" was used, and investigation of microhardness was done by Remet HX 1000. The three-point bend test was produced by "Shimadzu" AG-5kNX, Charpy impact V-notch test was performed by Instron 450MPX, 2D and 3D computer tomography were performed

Table 1 Chemical composition of specimen (wt%)

Sample no. /composition	C	Si	Mn	S	P	Cr	Ni	Ti	As	Cu
1	<0.12	<0.80	<2.00	<0.020	<0.035	17.0–19.0	9.0–11.0	<1.00		
2, 3	0.14–0.22	0.15–0.30	0.40–0.65	<0.050	<0.040	<0.30	<0.30		<0.080	<0.30
4, 5	<0.12	0.50–0.80	1.3–1.7	<0.030	<0.035	<0.30	<0.30	–	<0.080	<0.30

Table 2 Welding parameters

	v_1 (mm/s)	P (kW) First pass, without wobbling	v_2 (mm/s)	P (kW) Second pass, with wobbling	Amplitude (mm)	Frequency (Hz)
1	10	7	10	7	5	15
2	36	12,5	8	3	3	8
3	24	9	10	3	3	10
4	15	8	8	3,5	3	8
5	20	9	8	4	3	10

Sample no. 1, both pass wobbling of laser beam

v_1 welding speed of the first pass (mm/s), v_2 welding speed of the second pass (mm/s), P power of laser emission of the first and second pass, respectively (kW), *amplitude* amplitude of laser beam movement (mm), *frequency* frequency of laser beam movement (Hz)

with "North Star Imaging" XView CT X5000. The microhardness measurement was done for cap, middle, and root side of the weld joint. Three-point bend was used to test the plasticity of different sides of the specimen and of the cap and root sides.

3 Results and discussion

3.1 Visual control and metallographic analysis

Figure 2 shows the curve of sample 2; at the edges of welding seam wobbles of scanning trajectory of laser beam are observed, and the width of the seam is bigger than that of the original laser beam welding without wobbling. The photograph of the cap and root sides of a seam is presented in Fig. 3.

Figure 3 shows the quality of the surface of welding seam of samples 1–5. The width of the seam of sample 1 at cap and root sides is equal because two-sided welding with the same parameters of the process was used. Sample 2 does not have a full penetration from the root side, which is consistent with the image of cross-section (Fig. 4); sample 3 has some pores from the root side. Samples 4 and 5 have a good surface of the cap and root sides.

The cross-sections presented in Fig. 4 shows the interrelation of the width and depth of the second pass that depend on the emission power, amplitude, and frequency of the laser beam. It is seen that the first pass weld pool—samples 2–5—is smaller in width in comparison with the upper part, due to the fact that during wobbling of the second pass, a large weld pool is formed.

3.2 Metallographic analysis

Research of the microstructure of welded joints was carried out on samples 4 and 5, which are of the highest quality and have full penetration and good appearance. To investigate the microstructure of welded joints, photos were taken with a magnification of ×50 from the seam line of the transition to the base metal first pass without wobbling, and photos and line transition from the weld to the base metal of the second pass wobbling. Comparison of the microstructure of the base metal, HAZ, welds, and the first and second passes was performed at magnification of ×200.

Figure 5a shows the microstructure of the transition line seam–HAZ–base metal (from left to right) of the second pass with wobbling of samples 4 and 5; it is shown that the directional solidification of the weld metal and heat-affected zone is not significantly different. Figure 5b also shows the transition line seam–HAZ–base metal (from left to right) of the first pass without wobbling of the samples 4 and 5; the samples did not differ significantly.

Minor change of power settings and wobbling does not significantly affect the structure and mechanical properties of the HAZ and weld, except for a slightly smaller HAZ of the sample 4 (Fig. 5a, b) in comparison with the sample 5.

In addition, there is a difference in the size of the weld pool of the first (Fig. 5a) and second passes (Fig. 5b), since the first pass is received on more severe conditions without wobbling, and the second pass was on a softer mode with wobbling of laser beam. Figure 5b shows directional solidification of the weld metal towards the center, and Fig. 5a towards the center
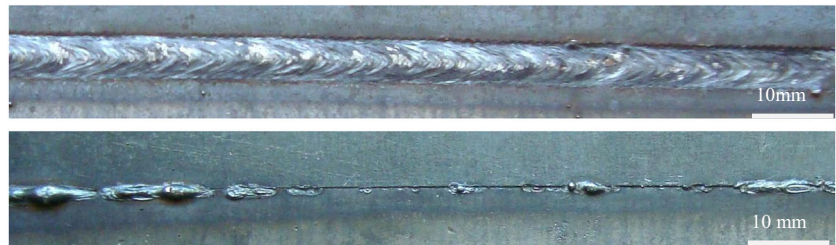
Fig. 2 Cap surface of sample no. 2

10 mm

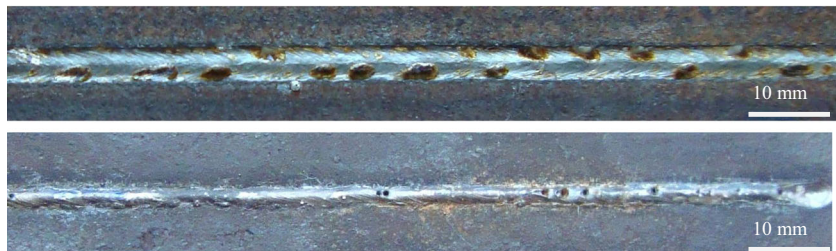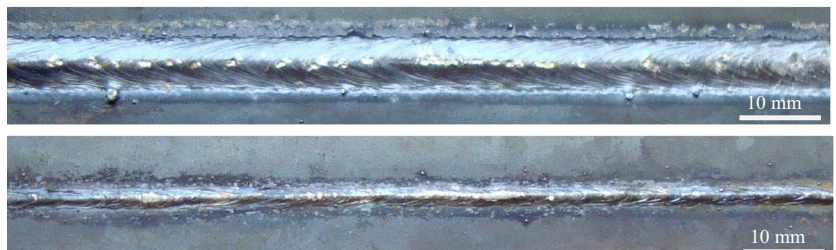**Fig. 3** The photograph of cap side and root side of welding seam
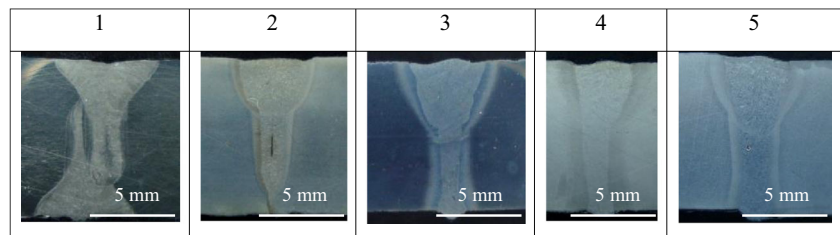
Sample 1
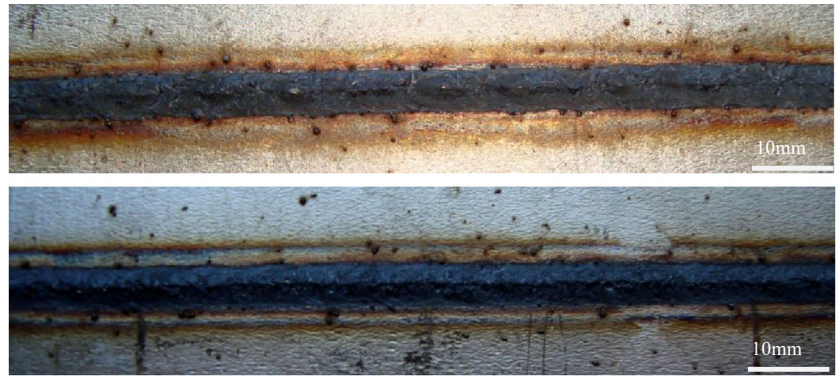
Sample 2

Sample 3

Sample 4
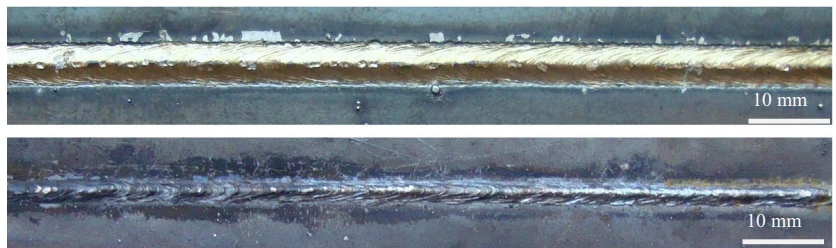
Sample 5

Fig. 4 The cross-section of sample nos. 1–5

1	2	3	4	5

and upwards, which is due to the direction of the heat sink and the impact on the plasticity of root and face joint (Table 4).

Figure 6a–d contains photographs of the microstructure of the base metal, HAZ, seam of samples 4 and 5 at magnification of ×200. In the photos, there are no significant differences between the relevant parts of the joints. The second pass is performed under the lower cooling rates, resulting in a more ductile weld metal structure in the second pass and in intermediate part between the first and second passes.

Figure 6 shows that there are only a few differences in the photograph of the seam (Fig. 6a–d, seam), which is likely due to the different heat input and different cooling rates of the weld metal; this difference in the modes did not considerably affect HAZ (Fig. 6a–d, HAZ).
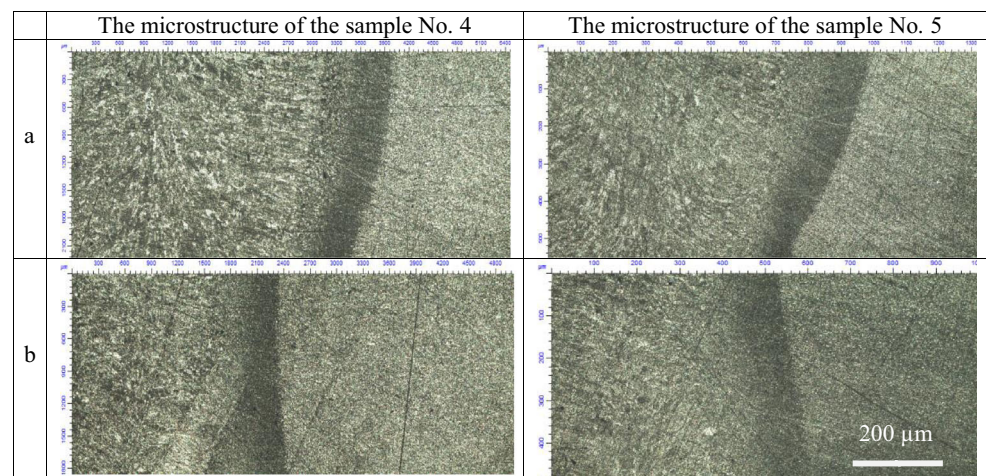
3.3 Mechanical properties

The impact of mechanical properties has been investigated by microhardness, three-point bend test, and Charpy impact V-notch test at the room temperature of the base material and weld. The results of microhardness measurement show that, in most cases, level values of the root side are higher than those of the middle and cap side, which is usual for laser welding (Table 3) [2, 5]. The second welding pass with wobbling mode

has more heat input due to lower speed and bigger welding pool, respectively, lower volume of microhardness. The second welding pass has annealing influence on the middle and root part of welding seam, which leads to decreasing microhardness for all parts of the welding seam.
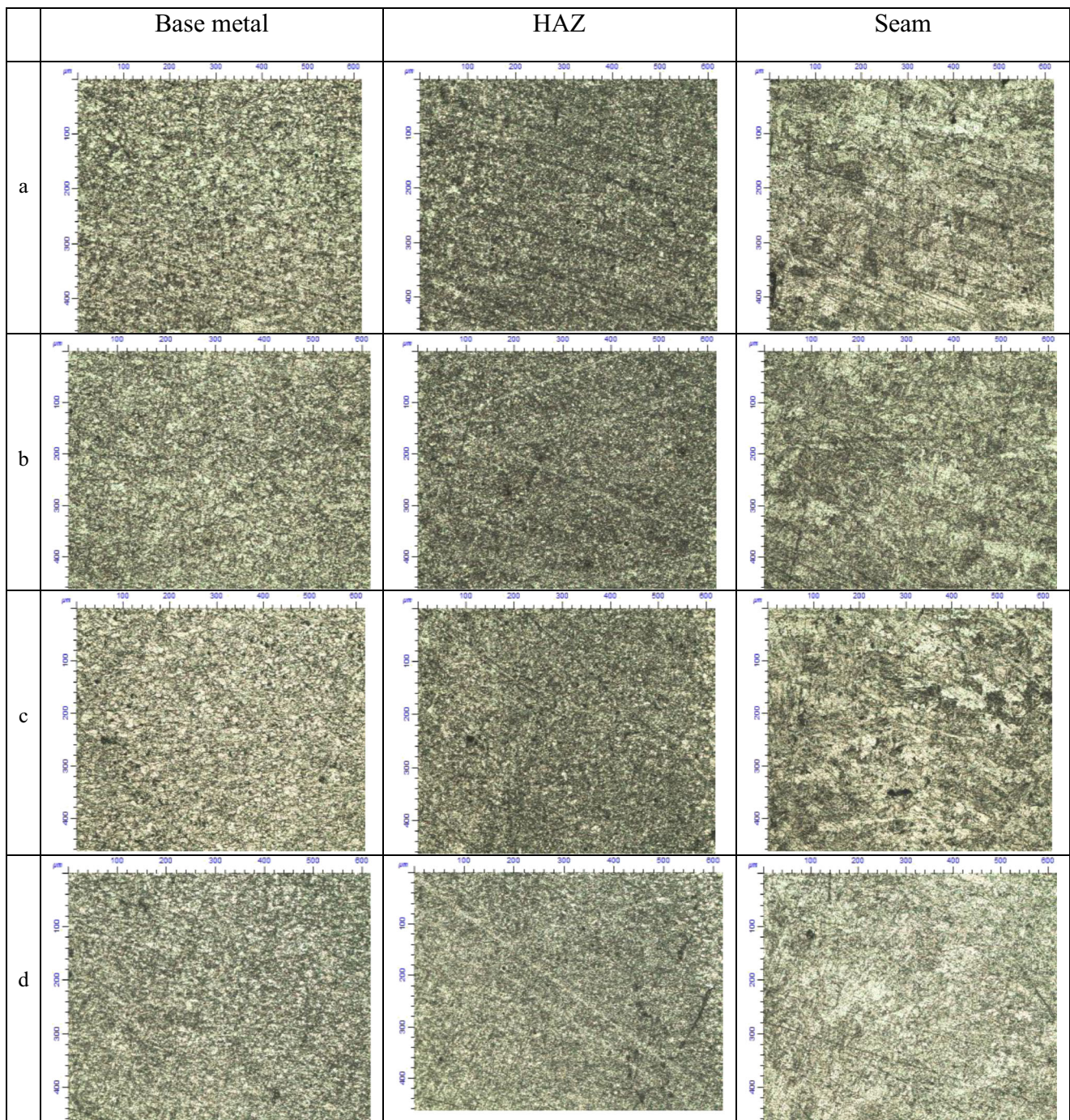
To investigate the level of plasticity, the three-point bend with load from cap side and root side has been used; the results are presented in Table 4. In most regulations, the normal bend angle for arc welding of similar thickness is 95–105°; in case of the laser welding, it is 40–80°—this is a very high value of plasticity for the welded joint (Fig. 7).

The Charpy impact V-notch test was done at 20 °C. The samples of the weld metal have a notch on the cap side of the joint, i.e., on the surface of the second pass with wobbling, the samples of the base metal have a notch in the same direction as that of the welded joint. Test results are presented in Fig. 8. Sample 1 has low values of impact toughness of weld metal, which is less than that of the base metal due to many large pores (Fig. 9). Sample 2 has also low values of impact toughness of weld metal due to defects like no full penetration and pores (Fig. 10). Samples 3–5 have values of impact toughness of weld metal lower when compared to the base metal that is due to the fact that the metal of the second welding pass with wobbling has a more coarse-grained structure compared with the base metal.

Fig. 5 The transition line of the first and second weld passes of sample nos. 4 and 5, magnification ×50. **a** Second pass with wobbling. **b** First pass without wobbling

The microstructure of the sample No. 4	The microstructure of the sample No. 5

	Base metal	HAZ	Seam
a			
b			
c			
d			

Fig. 6 The microstructure of base metal, HAZ, seam of the first and second weld passes of sample nos. 4 and 5, magnification of ×200. **a** Microstructure of the second pass with wobbling, sample no. 4. **b** Microstructure of the second pass with wobbling, sample no. 5. **c** Microstructure of the first pass without wobbling, sample no. 4. **d** Microstructure of the first pass without wobbling, sample no. 5

Table 3 The microhardness of different parts of welding seam and the base metal

Sample no.	Base metal, HV1 (MPa)	Cap, HV1 (MPa)	Middle, HV1 (MPa)	Root, HV1 (MPa)
1.	2700–3000	3100–3500	3000–3200	2800–3100
2.	1700–2000	2500–2800	2300–2500	3100–3400
3.	1700–2000	3100–3700	2300–2700	3500–3800
4.	2300–2500	2000–2500	2300–2500	2600–2900
5.	2300–2500	2100–2400	2100–2300	2600–2900

Table 4 The bend angle of samples

Sample	1	2	3	4	5
Base material	35°	40°	40°	45°	45°
Load, cap side	40°	50°	47°	45°	80°
Load, root side	38°	50°	55°	70°	45°
Destruction root surface	No	Yes	Yes	No	Yes
Destruction cap surface	No	Yes	Yes	Yes	No
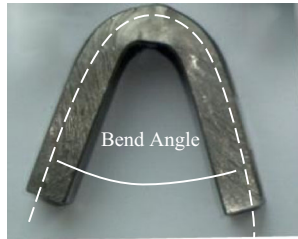
Fig. 7 Schematic view of bend angle

3.4 Computer tomography of welded joints

For a more thorough examination of welded samples, 2D and 3D computer tomography were used. 2D and 3D computer tomography were performed with "North Star Imaging" XView CT X5000. CT technology is X-raying of the obtained samples of X-ray range. 2D imaging can be used for express analysis, i.e., for detection of the presence or absence of large pores and defects in the form of fusions. For a more detailed analysis of the location and size of defects, 3D imaging can be applied, i.e., 3D model of the object can be formed. Note that the 3D imaging takes much more times and power, so only 2D imaging was applied to samples where large defects were revealed. 2D tomography of the sample 1 shows a lot of big pores (Fig. 9) at different depths of cross-section (2, 4, 6, and 8 mm), and sample 2 has some pores in the root part of seam and some cracks in the middle part of seam (Fig. 10), which agree with the cross-section in Fig. 4 and low values of Charpy impact V-notch test (Fig. 8).
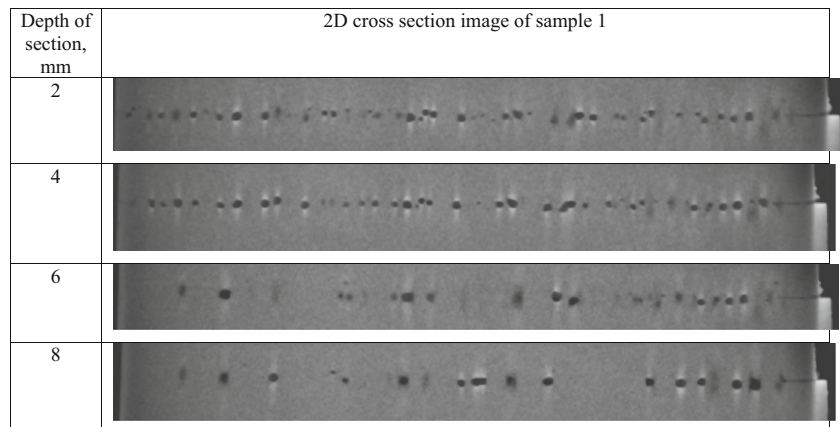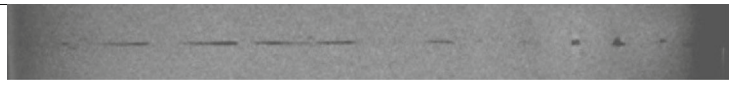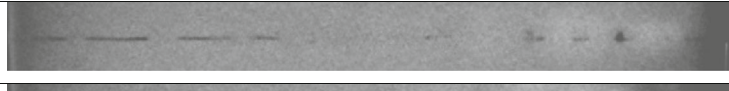
Fig. 8 Charpy impact V-notch test. *WS* welding seam, *BM* base metal

Fig. 9 2D computer tomography of sample 1

Depth of section, mm	2D cross section image of sample 1
2	
4	
6	
8	

Fig. 10 2D computer tomography of sample 2

Depth of section, mm	The 2D cross section image of sample 2
2	
6	
8	

3D computer tomography showed that samples 3–5 have no significant defects with a size more than 150–180 μm in the weld (Fig. 11). 3D imaging can be used for express analysis of the welded joints of critical parts in industrial production. Besides 3D imaging can be used to assess the quality of castings, depending on the power of the electron gun, solid thickness of the investigated metallic article can be up to 15–20 mm, and the minimum defect size is 50–70 μm. Objects of express analysis can be turbine blades, nozzles and welded joints, the size of which corresponds to the size of the imager camera.

Fig. 11 3D computer tomography of samples 3–5
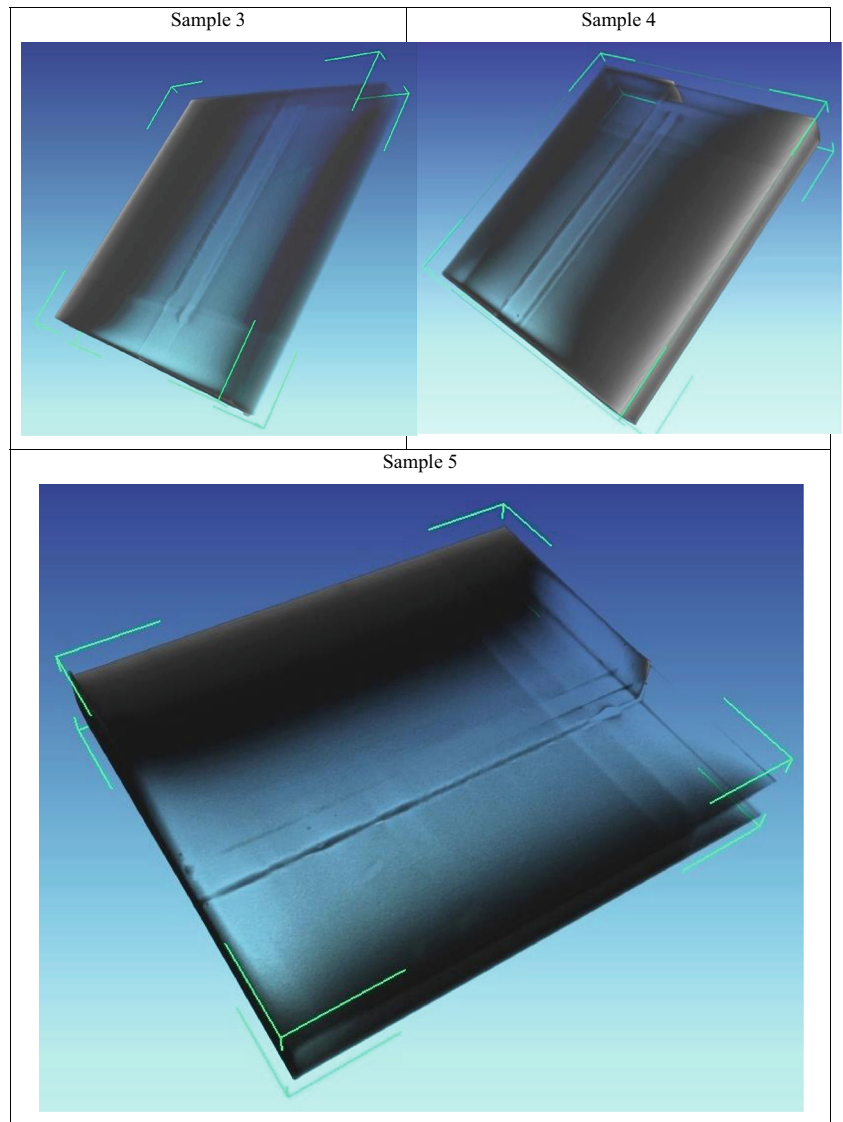
4 Conclusions

Special technical applications for laser welding will be improved infinitely. Nowadays, hybrid welding and bifocal beam laser welding are most popular. One of the newest applications is laser beam wobbling mode. It can be used for laser welding with filler material of large diameter, due to the large volume of the weld pool and healing defects of the first welding pass, increasing the ability to bridge workpieces with initial gap or low level of welding preparation, for welding big thickness workpiece by two to three passes with the use of low power laser beam. Besides this technology can be used for cladding process to provide bigger melting pool, it can help to reduce solidification speed, which is important in some cases.

In the present paper, the results of mechanical tests and metallographic investigations of weld joints, received by laser welding with the use of laser beam wobbling mode, were shown. Mechanical properties of weld joints are comparable to those of the base metal.

1. The influence of the second welding pass on the laser beam wobbling mode results in the decrease in microhardness of the cap and middle part of the seam, by annealing effect.
2. The toughness of samples 1–5 of the weld metal is about 50 % of the base metal due to the coarser structure of the weld metal.
3. Ductility of the weld joint is comparable to that of the base metal; however, the upper surface of the seam is more ductile than the surface of the root weld.
4. The second pass with wobbling of laser beam through lower cooling rates provides minimal number of phase transitions, which in turn guarantees less shrinkage and provides greater ductility of the weld metal.

References

1. Casalino G, Campanelli SL, Ludovico AD (2013) Laser-arc hybrid welding of wrought to selective laser molten stainless steel. Int J Adv Manuf Technol 68:209–216

2. Fersini M, Sorrentino S, Zilli G (2010) Duplex stainless steel for bridges construction: comparison between SAW and Laser-GMA hybrid welding. Weld World 5(5/6):2010

3. M. Merklein, A. Giera (2008) Laser assisted friction stir welding of drawable steel-aluminium tailored Hybrids Springer // ESAFORM 1299–1302

4. Westin, Stelling K, Gumenyuk A (2011) Single-pass laser-GMA hybrid welding of 13.5 mm thick duplex stainless steel. Weld World 55:39–49

5. Kristensen JK (2009) Thick plate CO_2-laser based hybrid welding of structural steels. Weld World 53(n° 1/2):48–58

6. Aalderink BJ, Pathiraj B (2010) Seam gap bridging of laser based processes for the welding of aluminium sheets for industrial applications. Int J Adv Manuf Technol 48:143–154

7. Gao M, Chen C, Mei S, Wang L, Zeng X (2014) Parameter optimization and mechanism of laser-arc hybrid welding of dissimilar Al alloy and stainless steel. Int J Adv Manuf Technol 74:199–208

8. Spottl M, Mohrbacher H (2014) Laser-based manufacturing concepts for efficient production of tailor welded sheet metals. Adv Manuf 2:193–202

9. Milberg J, Trautmann A (2009) Defect-free joining of zinc-coated steels by bifocal laser welding. Prod Eng Res Dev 3:9–15

10. Hayashi T, Matsubayashi K, Katayama S, Abe N, Matsunawa A, Ohmori A (2003) Reduction mechanism of porosity in tandem twin-spot laser welding of stainless steel. Weld Int 17(1):12–19

11. Yan J, Gao M, Li G, Zhang C, Zeng X, Jiang M (2013) Microstructure and mechanical properties of laser-MIG hybrid welding of 1420 Al-Li alloy. Int J Adv Manuf Technol 66:1467–1473

12. Yangchun Y, Wang C, Xiyuan H, Wang J, Shengfu Y (2010) Porosity in fiber laser formation of 5A06 aluminum alloy. J Mech Sci Technol 24(5):1077–1082

13. Chowdhury SH, Chen DL, Bhole SD, Powidajko E, Weckman DC, Zhou Y (2012) Fiber laser welded AZ31 magnesium alloy: the effect of welding speed on microstructure and mechanical properties. Metall Mater Trans A 43A:2133

14. Chen YB, Feng JC, Li LQ, Li Y, Chang S (2013) Effect of welding positions on droplet transfer in CO_2 laser-MAG hybrid welding. Int J Adv Manuf Technol 68:1351–1359

15. Chen Q, Wang Y Effect of heat treatment temperature on dissimilar welded joint. China Weld (Engl Ed) 22 (3):60–65

16. Lu F, Liu P, Ji H, Xu X, Gao Y (2014) Dramatically enhanced impact toughness in welded 10%Cr rotor steel by high temperature post-weld heat treatment. Mater Charact 92:149–158

17. Wang X-Y, Lei W-J (2011) Effect of postweld heat-treatment on microstructure and properties of 12Cr1MoVG/12Cr2MoWVTiB steel welded joints. Heat Treat Met 36(6):92–96

18. Liu W, Ma J, Atabaki MM, Pillai R, Kumar B, Vasudevan U, Sreshta H, Kovacevic R (2015) Hybrid laser-arc welding of 17-4 PH martensitic stainless steel. Lasers Manuf Mater Process 2(2):74-90

19. Fang C, Song Y, Wu W, Wei J, Zhang S, Li H, Dolgetta N, Libeyre P, Cormary C, Sgobba S (2014) The laser welding with hot wire of 316LN thick plate applied on ITER correction coil case. J Fusion Energy 33:752–758

20. Karhu M, Kujanpaa V, Lippold J et al (eds) (2011) Solidification cracking studies in multi pass laser hybrid welding of thick section austenitic stainless steel. Hot cracking phenomena in welds III. Springer-Verlag, Berlin